International Journal of Scientific Engineering and Science
Volume 8, Issue 8, pp. 1-7, 2024. ISSN (Online): 2456-7361

Detection of Iodide Using a Fluorescent Chemosensor Based on Quinaldinium and Imidazole Moieties

Ibrahim Uyanik[1*], Arwa Alsaleh[2]
[1]Metallurgical and Materials Engineering Department, Selçuk University, Konya, Türkiye-42075
[2]Chemistry Department, Selçuk University, Konya, Türkiye-42031
*Corresponding Author: ibrhm.uyanik@gmail.com

Abstract*—Here, the sensing capability of 2-(2-(1H-imidazol-5-yl)vinyl)-1-ethylquinolin-1-ium iodide (QIM) synthesized by the Knoevenagel reaction, was evaluated with certain anions (F^-, Cl^-, Br^-, I^-, CH_3COO^-, NO_3^-, HSO_4^-, and $H_2PO_4^-$) in solution phase of acetonitrile (MeCN) using fluorescence and absorption spectroscopy techniques. The fluorescence intensity of QIM was substantially quenched upon binding with I^- compared to other anions. The detection limit of QIM for I^- were calculated as 4.23 μM in MeCN, along with a linear range spanning from 0 μM to 50 μM. Further, the binding mechanism of QIM for detecting I^- ion was investigated through Job's plot analysis, and Benesi-Hildebrand study. Job's plots revealed that QIM formed complex with I^- in the ratio of 1:1. The binding constant for the QIM-I^- complex was determined to be 4.79×10^5 M^{-1} by Benesi-Hildebrand equation. Additionally, Stern Volmer quenching constant for the QIM-iodide interaction was determined as 0.0211×10^6 M^{-1}.*

Keywords*—Cationic sensor; fluorescent quenching; iodide; on/off sensing*.

I. INTRODUCTION

Development of molecular receptors capable of selectively detecting and quantifying specific analytes has become an increasingly important area of research for many years. One of the growing research areas in supramolecular chemistry that researchers have focused on is the recognition of anions with an appropriate receptor [1]. Iodide (I^-), as one of the halide anions, is an essential nutrient for the human body. It is an essential component of thyroid hormones, which regulate metabolism and play a vital role in growth and development. Additionally, I^- is involved in the development and maintenance of a healthy immune system. Many diseases are closely associated with I^- imbalances, such as iodine deficiency disorders and thyroid diseases. Furthermore, excessive exposure to iodine can have detrimental effects on the environment. Excessive release of I^- into aquatic ecosystems, primarily through industrial processes and the improper disposal of iodine-containing compounds, can lead to various environmental concerns such as bioaccumulation in aquatic organisms, disruption of aquatic ecosystems, and even contamination of drinking water sources. Additionally, the atmospheric deposition of iodine can contribute to the contamination of soils and plants [2–5]. Overall, I^- ions play a pivotal role in various scientific disciplines, including materials science, environmental monitoring, and analytical chemistry, highlighting their significance in shaping material properties, environmental assessment, and biological processes. Therefore, in recent years, there has been an increasing interest in developing a selective and sensitive method for the detection of I^- [6]. Current techniques for the detection of I^-, such as capillary electrophoresis [7], inductively coupled plasma mass spectrometry [8], ion chromatography [9], high-performance liquid chromatography [10], and gas chromatography-mass spectrometry [11], often require sophisticated instrumentation, lengthy sample preparation, and skilled personnel. To address these limitations, there is a need for the development of simple, rapid, and cost-effective analytical methods for I^- detection. Fluorescent chemosensors offer a promising approach for I^- sensing due to their high sensitivity, specificity, and ease of operation. Various chemosensors have been developed for the detection of I^- as reported in the literature, yielding significant findings. However, research endeavours in this area persist, focusing particularly on advancing sensing parameters including selectivity, enhanced sensitivity, reliability, and reusability. In the literature, the most efficient optical receptors for I^- sensing contain arrays of hydrogen bond donors such as imidazolium, quinolinium, acidified amide groups, triazole, and boronic acid [12–14]. Specifically, quinolinium derivatives have numerous uses in sensing and molecular recognition. They are employed as intercalators, fluorescent pH sensors, and signalling components in receptors. Furthermore, the quinoline moiety and especially quinolinium salts utilized to design various chemosensors have been found to exhibit strong interactions with anions such as halide ions, leading to a decrease in fluorescence intensity. This makes quinoline-based sensors highly sensitive and selective for halide ion detection [15–21]. I^- is known to efficiently quench the fluorescence of certain fluorophores through a heavy atom effect, providing a basis for the design of fluorescent I^- sensors [22–25]. In this respect, quinolinium salts have emerged as attractive fluorescent sensing platforms due to their ease of synthesis, high fluorescence quantum yields, and strong responses to analyte binding [26]. In this paper, we present the application of the quinolinium-based fluorescent sensor QIM for selectively detecting I^- over different anions such as fluoride, chloride, bromide, acetate, nitrate, hydrogen sulphate, and dihydrogen phosphate via fluorescence quenching.

II. MATERIALS AND METHODS

^1H and ^{13}C NMR spectra were recorded on a Bruker 400 MHz spectrometer using DMSO-d_6 solvent. FT-IR spectra were obtained using a Brucker Vector 22 FTIR spectrometer. Absorbance spectra were recorded on a Perkin Elmer Lambda-

35 UV-visible double beam spectrophotometer with standard 1.00 cm quartz cells, and fluorescence measurements were carried out on a PerkinElmer LS 55 spectrophotometer at room temperature. All reagents, chemicals, and solvents used in the experiments, unless otherwise specified, were obtained from commercial suppliers and utilized without further purification.

A. Synthesis and characterization of the probe QIM

The probe QIM was synthesized in a step process, as shown in Figure 1. The process involved refluxing 1-Ethylquinolinium iodide (1.00 g, 3.34 mmol) in 40ml of [$CHCl_3$:CH_3OH (1:4)] with piperidine for 10 minutes. Subsequently, 1H-imidazole-5-carbaldehyde (0.32g, 3.34 mmol) was added and the mixture was refluxed for 48 hours. Upon completion, as confirmed by TLC, the solvent of the fully mixed solution was completely evaporated using an evaporator and the resulting product was precipitated with methanol-diethyl ether. The product obtained was then dried under vacuum (yield; 77%, m.p. 235–236 °C). Anal. Calc. for $C_{16}H_{16}IN_3$: C, 50.89%: H, 4.24%: I, 33.64%: N, 11.13%). Anal. Found: C, 50.49%: H, 4.21%: I, 32.98%: N, 11.08%. ^{1}H-NMR (400 MHz, DMSO-d_6, 25 °C): δ (ppm) 1.59 (t, 3H, J= 7.3 Hz, CH_3), 5.01 (q, 2H, J= 7.3 Hz, CH_2), 7.61 (d, 1H, J= 15.3 Hz, CH=CH), 7.85 (bs, 1H, CH-im), 7.91 (t, 1H, Q-H), 8.01 (bs, 1H, CH-im), 8.15 (t, 1H, Q-H), 8.32 (m, 1H, Q-H and 1H, CH=CH), 8.52 (d, 1H, Q-H), 8.56 (d, 1H, Q-H), 8.96 (d, 1H, Q-H), 12.79 (s, 1H, NH-im). ^{13}C-NMR (100 MHz, DMSO-d_6, 25 °C): δ (ppm) 1160.7, 148.6, 143.2, 140.1, 135.6, 133.9, 132.8, 125.8, 123.9, 118.9, 51.6, 19.1. FT-IR (KBr) υ (cm^{-1}): 3418 (N-H), 3057 (Ar C-H), 1595 (C=C), 1348 (Ar C-N), 1150 (C-N).

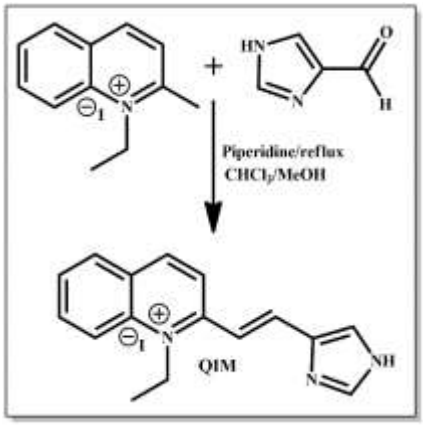

Fig. 1. Schematic representation of the synthesis route for QIM.

B. General procedure of spectroscopic studies

A stock solution of QIM (1.00 mM) was prepared in MeCN and diluted as necessary. Additionally, stock solutions of anions (F^-, Cl^-, Br^-, I^-, CH_3COO^-, NO_3^-, HSO_4^- and $H_2PO_4^-$) (1.0 mM) were prepared by dissolving appropriate amounts of their corresponding tetrabutylammonium salts in MeCN. The test solutions for fluorescence and absorbance spectra were prepared by initially including 30 μL of QIM solution in a test tube, succeeded by adding a suitable portion of each anion stock solution, and further diluting the mixture to reach a total volume of 3.0 mL. This identical method was applied to both fluorescence titration and interference investigations involving QIM-I^- complexes within a solution alongside other ions. Fluorescence intensity readings were conducted at 250 nm and 377 nm excitation and emission wavelengths, respectively. To ensure consistency, every measurement was repeated twice, and a sufficient interval was allowed before recording each spectrum to guarantee the evenness of the solution.

III. Results and Discussion

A. Synthesis and Characterization

The Knoevenagel condensation is a significant chemical reaction involving the reaction of aldehydes with active methylene compounds. This conversion has broad application potential in organic synthesis and serves as a fundamental method for producing fine chemicals and heterocyclic compounds of biological importance. In this work, the chemical sensor QIM was synthesized through the Knoevenagel condensation. Its characterization was effectively conducted through FT-IR, ^{1}H NMR, and ^{13}C NMR analyses. The disappearance of the signal of the aldehyde proton (1H-imidazole-5-carbaldehyde) at 9.75 ppm and the observation of olefin protons at 7.61 and 8.32 ppm confirmed the formation of QIM.

B. Solvent Effect

To determine the maximum absorbance of the receptor QIM in various solvents, UV-Vis spectrometric studies were conducted using $CHCl_3$, DCM, THF, EtOH, MeOH, MeCN, DMF, and DMSO. Interestingly, the maximum longwave λ_{max} remained consistent across all solvents, with no discernible differences in the absorbance of the receptor. Taking into account factors such as solubility, volatility, and miscibility with H_2O, MeCN was selected as the solvent system for the subsequent sensing studies.

C. Iodide Sensing Ability of QIM: Fluorescence and UV-Vis Studies

UV-vis and fluorescence spectroscopy were used to study the interaction between QIM molecule and certain anions (F^-, Cl^-, Br^-, I^-, CH_3COO^-, NO_3^-, HSO_4^-, and $H_2PO_4^-$) in MeCN. The maximal absorbance in the absorption spectrum of the free ligand QIM is observed at 280 nm, as can be seen in Fig. 2a. Upon the introduction of various anions (100 μM) into the free ligand solution (10 μM), a decrease in the intensities of the principal absorbances is noted, implying the occurrence of interactions between the ligand and these anions. Notably, upon the addition of I^- as an external analyte into the QIM solution, a notable disappearance of the maximal absorbance of the probe is observed, concomitant with the emergence of a novel absorption peak centered at approximately 450 nm. This discernible red shift in the absorption spectrum indicates a substantial alteration in the electronic structure or local environment of the ligand induced by its interaction with I^-.

Based on previous studies, the quenching of fluorescence in a cationic fluorescent ligand can be induced by the presence of I^- as the counterion [27]. The significance of counter anions, such as I^- for our sensor system, in influencing the emission properties of cationic probes in various states, whether in a condensed phase or solution, should be emphasized. In MeCN,

QIM molecules typically exist as ion pairs (cation and I^- ion) that are solvent-separated.

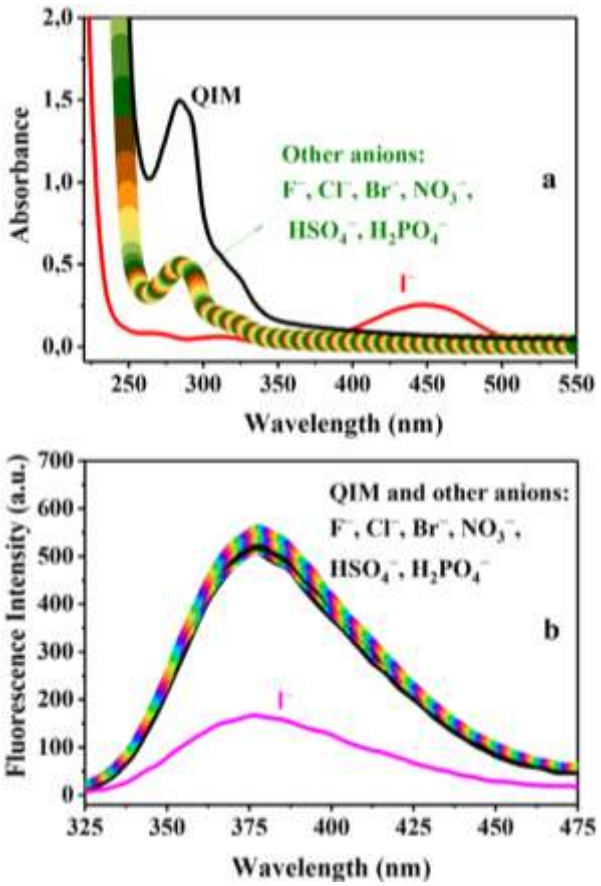

Fig. 2. Absorption (a) and emission (b) spectra of probe QIM (10 μM) in the presence of different anions (100 μM) in MeCN solution.

This particular molecular arrangement reduces collisions and hinders the quenching influence of I^- as counter ion, suggesting that I^- does not intrinsically quench the fluorescence of QIM. It is postulated that the fluorescence of cationic QIM may decrease upon the introduction of I^- salt as an analyte, resulting in a quenching effect on fluorescence due to the accelerated intersystem crossing process, leading to non-radiative relaxation through collisions with QIM molecules. Consequently, we further investigated the fluorescence response of QIM towards I^- as an external analyte in a solution medium. Thus, to investigate the selectivity of QIM (10 μM) towards I^- over other anions in MeCN, fluorescent spectroscopy studies were conducted to analyze the fluorescence response of QIM to various anions, including F^-, Cl^-, Br^-, I^-, NO_3^-, $H_2PO_4^-$, and HSO_4^-, each at a concentration of 100 μM. The fluorescence emission profile of the probe QIM displayed a peak emission at 377 nm (with an excitation wavelength of 250 nm), as illustrated in Fig. 2b. Nevertheless, the introduction of only I^- into the QIM solution results in a significant decrease in fluorescence. Conversely, no substantial alterations or bit changes were noted in the fluorescence emission characteristics of the probe QIM in the presence of the other tested anions, underscoring the exceptional selectivity of QIM towards I^-. The effective fluorescence quenching ability of the iodide ions may be primarily attributed to the heavy-atom effect they exhibit by increasing the probability of non-radiative processes, such as collisional quenching or energy transfer. Additionally, the interactions between I^- and specific functional groups in the quinolinium or imidazole units of QIM may also contribute to fluorescence quenching. For example, I^- may interact with positively charged nitrogen atoms in the quinolinium unit or -NH groups in the imidazole moiety, leading to electron transfer processes that can quench fluorescence.

D. Fluorescence Titration Studies for I^- Sensing: Calibration Curve, Limit of Detection, and Stoichiometry

To evaluate the interaction between QIM and I^-, a fluorescence titration experiment, with an excitation wavelength of 250 nm, was performed 3 times in MeCN solution.

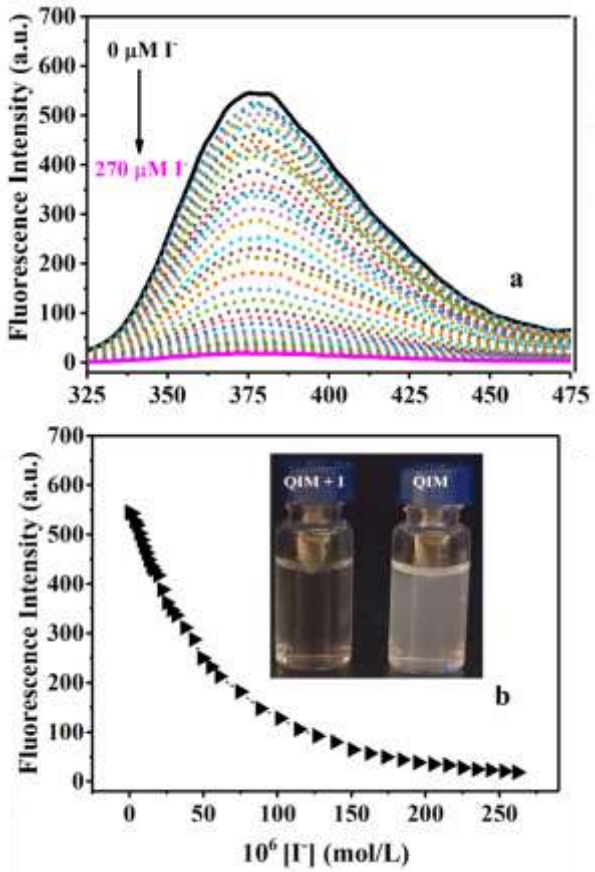

Fig. 3. Fluorescence intensity changes of the probe QIM (10 μM) in the presence of an increasing concentration of I^- in MeCN (a), the fluorescence intensity values at 377 nm of the QIM-I complex depending on the concentration of I^- (b). Photographs in the inset were taken under a UV lamp.

The results presented in Fig. 3a demonstrate a progressive reduction in the intensity of the fluorescence emission peak at 377 nm as the concentration of I^- was incrementally increased from 0.0 to 270 μM in the solution containing QIM. Subsequently, the fluorescence intensity of the QIM probe was nearly entirely quenched, exhibiting a quenching efficiency of 90%, following the introduction of 250 μM of I^- (Fig. 3b). This quenching phenomenon is attributed to both the heavy atom

International Journal of Scientific Engineering and Science
Volume 8, Issue 8, pp. 1-7, 2024. ISSN (Online): 2456-7361

effect and the intramolecular charge transfer (ICT) process. Moreover, a meticulous exploration of the time-dependent alterations in the fluorescence intensity of QIM at 377 nm was undertaken, given the imperative nature of real-time analyte determination in practical scenarios. Notably, it was observed that the fluorescence intensity of QIM exhibited a marked reduction within a brief span of 10 seconds after the introduction of 10 equiv. of I^- into the QIM solution (at a concentration of 10 μM) (Fig. 4).

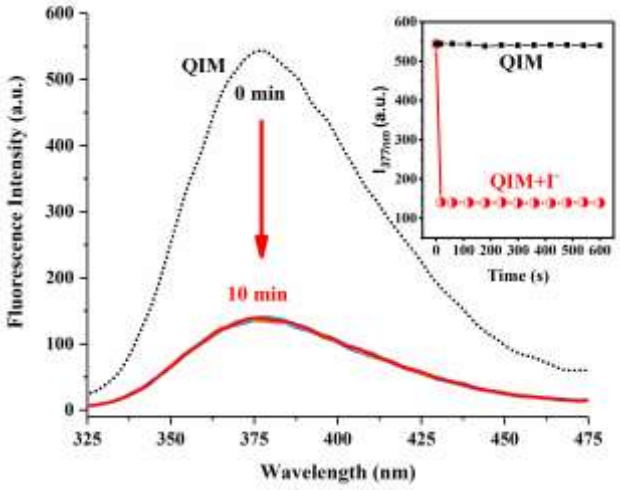

Fig. 4. Time-dependent fluorescence intensity of QIM (10 μM) in MeCN after the addition of 100 μM I–. The inset shows the change in fluorescence emission value of QIM and QIM-I– at 377 nm with time.

Furthermore, the fluorescence emission emanating from the QIM-I^- complex remained constant, thereby indicating the successful formation of the complex (as evidenced in Fig. 4 inset). Consequently, the inference drawn from these observations suggests that QIM manifests a rapid response rate and holds promise as a real-time probe for the detection of I^-. Moreover, when iodide ions are introduced into the QIM solution in MeCN under UV light, the original color of QIM vanishes. This phenomenon serves as evidence of the colorimetric detection ability of QIM towards iodide ions (Fig. 3 inset).

The fluorescence quenching effect of iodide ions on a fluorescent probe can be quantified using the Stern-Volmer equation, which allows for the determination of important parameters such as the quenching constant and the binding constant between the fluorescent probe and iodide ions. Thus, the assessment of fluorescence quenching efficiency was conducted through the utilization of the Stern–Volmer equation [28]:

$$\frac{F_0}{F} = 1 + K_{sv}[I^-]$$

Where F_0 represents the initial fluorescence intensity of QIM, F signifies the fluorescence intensity of QIM in the presence of a specific concentration of I^-.

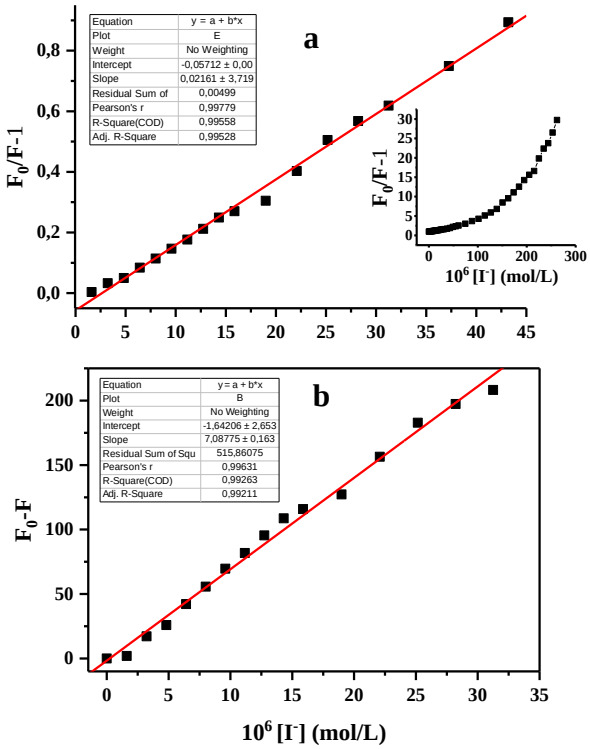

Fig. 5. Stern Volmer (a) and Calibration (b) plot of Fluorescence intensity changes of the probe QIM (10 μM) in the presence of an increasing concentration of I^- in MeCN (λex= 250 nm). The inset plot of (b) shows the change of F0/F-1 value in the 0-270 μM I^- range.

As depicted in Fig. 5a, the (F_0/F)-1 value approaching 1 exhibited a notably strong linear correlation (R^2 = 0.9953) across a concentration range spanning from 0 to 45 μM. Subsequently, the quenching constant (K_{sv}) was determined to be 0.0211×10^6 M^{-1}. Following the introduction of I^-, the emission intensity of QIM at 377 nm remains relatively unchanged, even in instances where the concentration of I^- reaches levels as high as 270 μM (refer to Fig. 3). I^- is recognized within scientific circles as a proficient quencher, operating based on the dynamic quenching mechanism involving collisions between the emitter and the quencher. However, at high concentrations of I^-, the positive deviation from linearity (Fig. 5a inset) suggests that iodine is causing both static and dynamic quenching effects. This indicates that the fluorescence quenching process involving iodine is complex and involves both types of quenching mechanisms simultaneously during the sensing. It is plausible to suggest that the combined influence of electrostatic interactions and vigorous collisions between QIM and quencher I^- likely underpins the notable fluorescence quenching observed. Additionally, the emission intensity at 377 nm demonstrates a strong linear correlation (R^2 = 0.993) with I^- concentrations ranging from 0.00 to 33.0 μM (Fig. 5b), and the detection limit (LOD) for I^- with QIM is estimated to be 4.23 μM based on the following equation:

$$LOD = 3\,sb/k$$

where *sb* is the standard deviation of the blank solution and k is the slope of the calibration curve. These findings indicate that QIM serves as a sensitive I^- sensor, enabling accurate

International Journal of Scientific Engineering and Science
Volume 8, Issue 8, pp. 1-7, 2024. ISSN (Online): 2456-7361

detection at low concentrations. The stoichiometric composition of the QIM-I⁻ complex was validated using Job's method, also known as the method of continuous variations. For this purpose, the solutions of equimolar concentration (1.5×10^{-5} M) of the two components are mixed in different ratios varying from 1:9 to 9:1. Fig. 6a displays a plot of absorbance (at 280 nm) against mole fraction (X), revealing a maximum absorbance approximately at 0.5, confirming a 1:1 stoichiometry for the QIM-I⁻ complex. Moreover, the analysis of emission spectra of QIM in conjunction with I⁻ unveiled a maximal emission at a mole fraction of 0.5 (at 377 nm). This observation also provides evidence supporting a 1:1 binding mode between QIM and I⁻, as illustrated in Fig. 6b.

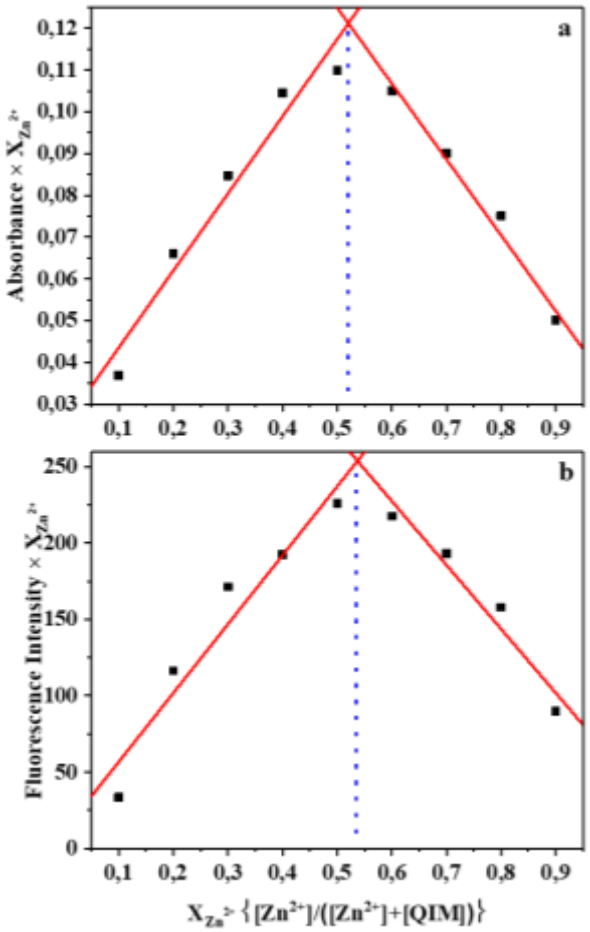

Fig. 6. Job's plot of the probe QIM with I– from (a) UV-vis spectral studies and (b) Fluorometric studies.

The Benesi-Hildebrand method is frequently employed to characterize the interaction between a sensor and an analyte. This method enables the determination of the binding constant (*Ka*) and the number of binding sites (n) by the equation [29, 30]:

$$\log(F_0 - F)/F = \log K_a + \mathrm{n}\log[I^-]$$

where, in the absence and presence of various concentrations of I⁻, the fluorescence intensities of QIM are denoted by F_0 and F, respectively. The graph of log $(F_0\text{-}F)/F$ versus log [I⁻] is depicted in Fig. 7. The calculated values of K_a and n from the linear plot in Fig. 6 were determined to be 4.79×10^5 M^{-1} and 1.3, respectively. The value of n was close to 1.0, indicating the presence of one binding site and one coordinating site on QIM. The binding constant value affirmed the existence of a strong binding interaction between QIM and I⁻.

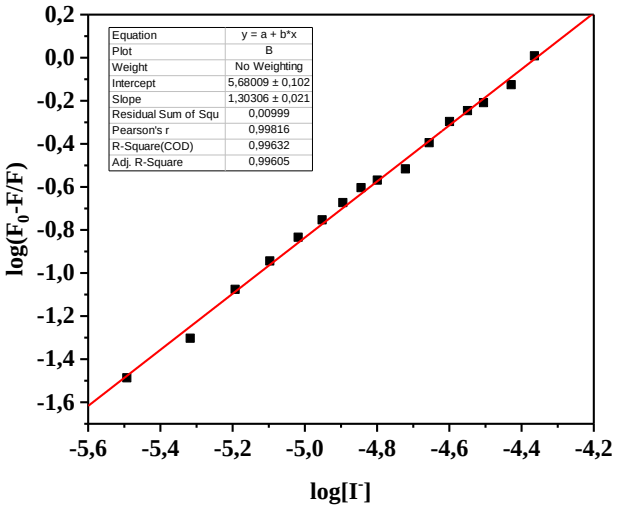

Fig. 7. Benesi Hildebrand curve from the fluorescence intensity data of QIM (10 μM) with different concentrations of Zn2+.

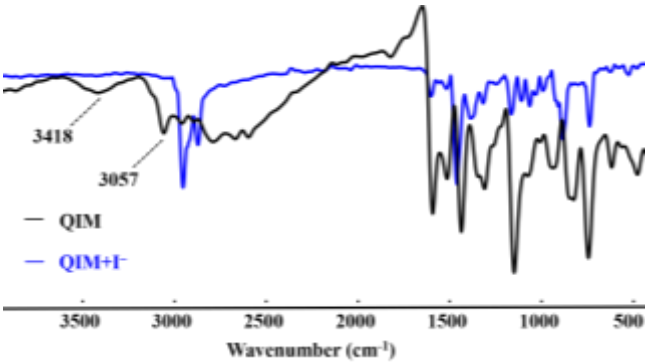

Fig. 8. Comparative FT-IR spectra of QIM and QIM-I⁻ complex (1×10^{-5} M).

E. FT-IR Studies

The confirmation of the interaction between QIM and I⁻ was established through the utilization of FT-IR spectroscopy. In the FT-IR analysis, an equimolar mixture of QIM-I was prepared in MeCN and stirred for 30 minutes at ambient temperature. Subsequently, the solvent was evaporated under reduced pressure, and the resulting solid residue was dried. Following the formation of the complex, the FT-IR spectrum of QIM (Fig. 8) exhibited discernible changes including shifts, disappearance, and emergence of new bands. Notably, significant alterations were observed in the spectral range of 3500–2000 cm^{-1}, where the peaks at 3418 cm^{-1} (N-H) and 3057 cm^{-1} (aromatic C-H) were absent. Based on these findings, it can be inferred that the N-H and C-H functional groups within the imidazole moiety of QIM likely contribute to the interaction between QIM and I⁻ (Fig. 9).

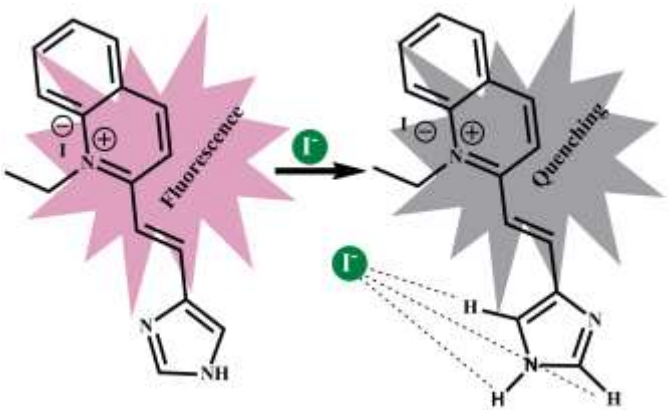

Fig. 9. Proposed interaction mechanism between QIM and iodide.

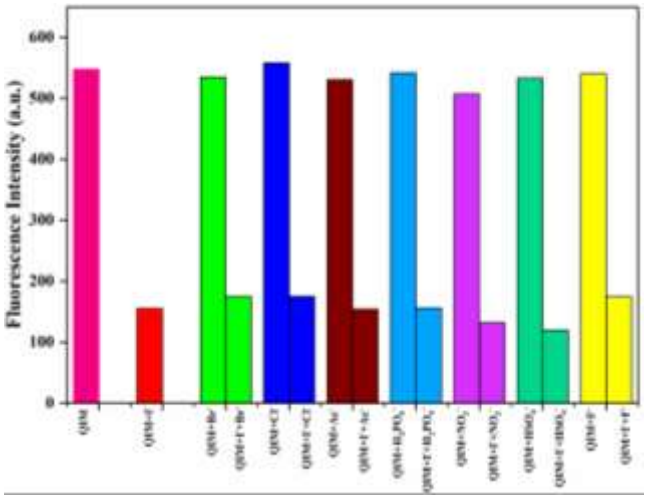

Fig. 10. Fluorescence intensities of probe QIM (10 μM) in the absence and presence of I^- ions (100 μM) and different interfering anions including F^-, Cl^-, I^-, NO_3^-, $H_2PO_4^-$, and HSO_4^- (100 μM) in MeCN at λ_{em}= 377 nm.

F. Competition Studies

Competition experiments play a crucial role in understanding the performance of the probe QIM in complex sample matrices and can help in optimizing its design for specific applications. Additionally, the sensitivity of the probe towards the target analyte can be assessed by comparing the fluorescence signals at different concentrations of the analyte. Thus, to evaluate the potential interference of other anions such as F^-, Cl^-, Br^-, NO_3^-, $H_2PO_4^-$, and HSO_4^-, the fluorescence response of QIM to I^- in the presence of the aforementioned anions at a concentration of 100 μM was investigated, as illustrated in Fig. 10. The findings demonstrate that even in the presence of equimolar concentrations of other anions, the addition of I^- leads to a significant quenching of fluorescence, thereby confirming the high anti-interference capability of QIM with I^-. The results of these competition experiments can provide valuable insights into the practical applications of the probe QIM. For example, the ability of the probe to selectively detect the target analyte in the presence of other interfering anions can determine its usefulness in real-world scenarios.

IV. CONCLUSION

In conclusion, the chemosensor 2-(2-(1H-imidazol-5-yl)vinyl)-1-ethylquinolin-1-ium iodide (QIM) based on quinolinium and imidazole moieties has been utilized for the selective detection of iodide. Upon the introduction of I^- salt into the solution of QIM, substantial alterations were observed in both its absorption and emission spectra. Specifically, in the presence of I^-, the fluorescence spectra of QIM showed a notable decrease in fluorescence intensity (fluorescence quenching) compared to other anions. The sensor exhibits excellent selectivity towards iodide over other anions. Lastly, we hope that this fluorescent sensor can contribute to the development of simple, rapid, and cost-effective analytical methods for iodide detection in various applications.

ACKNOWLEDGMENT

The authors express their gratitude to the Chemistry Department, Selcuk University, Konya, Türkiye for using their facilities to conduct the research analyses.

REFERENCES

[1] P. A. Gale and C. Caltagirone. “Fluorescent and colorimetric sensors for anionic species,” *Coord. Chem. Rev*., vol. 354, pp. 2–27, 2018.
[2] G. Medeiros-Neto. “Iodine deficiency disorders,” *Thyroid*, vol. 1, issue 1, pp. 73–82. 1990.
[3] S. Venturi. “Is there a role for iodine in breast diseases,” *Breast*, vol. 10, issue 5, pp. 379–382, 2001.
[4] F. Delange. “The role of iodine in brain development,” *Proc. Nutr. Soc*., vol. 59, issue 1, pp. 75–79, 2000.
[5] A. M. Leung and L. E. Braverman. “Consequences of excess iodine,” *Nat. Rev. Endocrinol*., vol. 10, pp. 136–142, 2014.
[6] M. Mansha, S. A. Khan, Md. A. Aziz, A. Z. Khan, S. Ali, and M. Khan. “Optical chemical sensing of iodide ions: a comprehensive review for the synthetic strategies of iodide sensing probes, challenges, and future aspects,” *Chem. Rec*., vol. 22, issue 7, e202200059, 2022.
[7] A. N. D. Macedo, K. Teo, A. Mente, M. J. McQueen, J. Zeidler, P. Poirier S. A. Lear, A. Wielgosz, and P. Britz-McKibbin. “A robust method for iodine status determination in epidemiological studies by capillary electrophoresis,” *Anal. Chem*., vol. 86, issue 20, pp. 10010–1015, 2014.
[8] T. I. Todorov, T. Smith, A. Abdalla, S. Mapulanga, P. Holmes, M. Hamilton, T. Lewis, and M. McDonald. “Comparison of ICP-MS and spectrophotometry methods for the analysis of iodine in 2013 US FDA total diet study samples,” *Food Anal. Methods*, vol. 11, pp. 3211–3223, 2018.
[9] N. Gros. “Ion chromatographic analyses of sea waters, brines and related samples,” *Water*, vol. 5, issue 2, pp. 659–676, 2013.
[10] M. Tatarczak-Michalewska, J. Flieger, J. Kawka, W. Flieger, and E. Blicharska. “HPLC-DAD determination of iodide in mineral waters on phosphatidylcholine column,” *Molecules*, vol. 24, issue 7, pp.1243–1256, 2019.
[11] J. W. Dorman and S. M. Steinberg. “Analysis of iodide and iodate in Lake Mead, Nevada using a headspace derivatization gas chromatography–mass spectrometry,” *Environ. Monit. Assess*., vol. 161, pp. 229–236, 2010.
[12] AE Z. Xu, S. K. Kim, and J. Yoon. “Revisit to imidazolium receptors for the recognition of anions: highlighted research during 2006–2009,” *Chem. Soc. Rev*., vol. 39, pp. 1457–1466, 2010.
[13] W. Sun, S. Guo, C. Hu, J. Fan, and X. Peng. “Recent development of chemosensors based on cyanine platforms,” *Chem. Rev*., vol. 116, issue 14, pp. 7768–7817, 2016.
[14] R. Badugu, J. R. Lakowicz, and C. D. Geddes. “Anion sensing using quinolinium based boronic acid probes,” *Curr. Anal. Chem*., vol. 1, issue 2, pp. 157–170, 2005.
[15] T. Saleem, S. Khan, M. Yaqub, M. Khalid, M. Islam, M. Y. ur Rehman, M. Rashid, I. Shafiq, A. A. C. Braga, A. Syed, A. H. Bahkali, J. F. Trant, and Z. Shafiq. “Novel quinoline-derived chemosensors: synthesis, anion recognition, spectroscopic, and computational study,” *New J. Chem*., vol. 46, issue 38, pp. 18233–18243. 2022.

[16] C. D. Geddes. "Optical halide sensing using fluorescence quenching: theory, simulations and applications - a review," *Meas. Sci. Technol*., vol. 12, no. 9, R53, 2001.
[17] C. D. Geddes. "Halide sensing using the SPQ molecule," *Sens. Actuators B: Chem*., vol. 72, issue 2, pp. 188–195, 2001.
[18] A. N. Swinburne, M. J. Paterson, A. Beeby, and J. W. Steed. "A quinolinium-derived turn-off fluorescent anion sensor," *Org. Biomol. Chem*., vol. 8, issue 5, pp. 1010–1016, 2010.
[19] I. Bazany-Rodríguez, D. Martínez-Otero, J. Barroso-Flores, A. K. Yatsimirsky, and A. Dorazco-González. "Sensitive water-soluble fluorescent chemosensor for chloride based on a bisquinolinium pyridine-dicarboxamide compound," *Sens. Actuators B: Chem*., vol. 221, pp. 1348–1355, 2015.
[20] R. Rautela, P. Arora, N. K. Joshi, S. Pant, and H. C. Joshi. "Fluorescence quenching of 8-methyl quinolinium: An efficient halide indicator mechanism," *J. Mol. Liq*., vol. 218, pp. 632–636. 2016.
[21] R. Badugu, J. R. Lakowicz, and C. D. Geddes. "A wavelength–ratiometric fluoride-sensitive probe based on the quinolinium nucleus and boronic acid moiety," *Sens. Actuators B: Chem*., vol. 104, issue 1, pp. 103–110, 2005.
[22] D. Y. Lee, N. Singh, M. J. Kim, and D. O. Jang. "Chromogenic and fluorescent recognition of iodide with a benzimidazole-based tripodal receptor," *Org. Lett*., vol. 13, issue 12, pp. 3024–3027, 2011.
[23] J. Chen, Q. Lin, Q. Li, W. T. Li, Y. M. Zhang, and T. B. Wei. "A highly selective colorimetric chemosensor for detection of iodide ions in aqueous solution," *RSC Adv*., vol. 6, issue 89, pp. 86627–86631, 2016.
[24] N. Alizadeh, A. Akbarinejad, S. Hosseinkhani, and F. Rabbani. "Synthesis of highly fluorescent water-soluble polypyrrole for cell imaging and iodide ion sensing," *Anal. Chim. Acta*, vol. 1084, pp. 99–105, 2019.
[25] P. Rani, J. Sindhu, and S. Kumar. "5-Hydroxydibenzo[a,i]phenazine-8,13-dione: A selective and sensitive colorimetric and fluorescent 'turn-off' sensor for iodide ion," *J. Mol. Struct*., vol. 1275, 134621, 2023.
[26] S. Panda, A. Jadav, N. Panda, and S. Mohapatra. "A novel carbon quantum dot-based fluorescent nanosensor for selective detection of flumioxazin in real samples," *New. J. Chem*., vol. 42, issue 3, pp. 2074–2080, 2018.
[27] R. X. Zhang, P. F. Li, W. J. Zhang, N. Li, and N. Zhao. "A highly sensitive fluorescent sensor with aggregation-induced emission characteristics for the detection of iodide and mercury ions in aqueous solution," *J. Mater. Chem. C*, vol. 4, issue 44, pp. 10479–10485, 2016.
[28] U. Krishnan, S. Manickam, and S. K. Iyer. "Turn-off fluorescence of imidazole-based sensor probe for mercury ions," *Sens. Diagn*., vol. 3, pp. 87–94, 2024.
[29] D. Sahoo, P. Bhattacharya, and S. Chakravorti. "Quest for Mode of Binding of 2-(4-(Dimethylamino)styryl)-1-methylpyridinium Iodide with Calf Thymus DNA," *J. Phys. Chem. B*, vol. 114, issue 5, pp. 2044–2050. 2010.
[30] H. A. Benesi and J. H. J. Hildebrand. "A Spectrophotometric Investigation of the Interaction of Iodine with Aromatic Hydrocarbons," *J. Am. Chem. Soc*., vol. 71, issue 8, pp. 2703–2707, 1949.